Activation of coherent lattice phonon following ultrafast molecular spin-state photo-switching: A molecule-to-lattice energy transfer

A. Marino,[1] M. Cammarata,[1] S. F. Matar,[2] J.-F. Létard,[2] G. Chastanet,[2] M. Chollet,[3] J. M. Glownia,[3] H. T. Lemke,[3] and E. Collet[1,a)]
[1]*Institute de Physique de Rennes, UMR 6251 University Rennes 1-CNRS, 35042 Rennes, France*
[2]*CNRS, Université de Bordeaux, ICMCB, 87 avenue du Dr. A. Schweitzer, Pessac 33608, France*
[3]*LCLS, SLAC National Laboratory, Menlo Park, California 94025, USA*

(Received 6 September 2015; accepted 9 November 2015; published online 20 November 2015)

We combine ultrafast optical spectroscopy with femtosecond X-ray absorption to study the photo-switching dynamics of the $[Fe(PM\text{-}AzA)_2(NCS)_2]$ spin-crossover molecular solid. The light-induced excited spin-state trapping process switches the molecules from low spin to high spin (HS) states on the sub-picosecond timescale. The change of the electronic state (<50 fs) induces a structural reorganization of the molecule within 160 fs. This transformation is accompanied by coherent molecular vibrations in the HS potential and especially a rapidly damped Fe-ligand breathing mode. The time-resolved studies evidence a delayed activation of coherent optical phonons of the lattice surrounding the photoexcited molecules.
[http://dx.doi.org/10.1063/1.4936290]

I. INTRODUCTION

Many chemical and biological systems can switch between different electronic and structural states within less than 1 ps under light excitation. Such transformations, as well as their recovery towards the stable state, involve not only the photoactive center with a molecular transformation but also its environment (Schoenlein *et al.*, 1991; Elsaesser and Kaiser, 1991; Barbara *et al.*, 1992; Rosspeintner *et al.*, 2013; Jun *et al.*, 2015; and Levantino *et al.*, 2015a; 2015b). For example, the energy transfer between a "hot" photo-excited molecule and its surrounding solvent is at the origin of molecular vibrational cooling and solvent heating. The light-control of molecular transformations expands nowadays towards materials science, offering new opportunities to impact the macroscopic state of materials with a light pulse (Koshihara, 2009). Molecular crystals are promising systems composed of many interacting elements which can give rise to collective transformations as ferroelectricity (Collet *et al.*, 2003; Okamoto *et al.*, 2004; and Uemura and Okamoto, 2010) or metal-insulator transitions for instance (Chollet *et al.*, 2005; Kawakami, 2009; Gao *et al.*, 2013; and Servol *et al.*, 2015). In such systems, the charge redistributions induced by light at the intra- and inter-molecular levels activate (through the couplings between charge and structural degrees of freedom) coherent optical phonons in the early stages of the transformation, which results from the energy redistribution from the absorbing centers to the molecular and lattice degrees of freedom.

Spin-crossover (SCO) materials belong to a family of prototypical systems showing photochromic and photo-magnetic responses between two competitive states of different spin multiplicities (Gütlich and Goodwin, 2004 and Halcrow, 2013). In the present case of study, Fe^{II}-based

a)Author to whom correspondence should be addressed. Electronic mail: eric.collet@univ-rennes1.fr

SCO complexes, of $3d^6$ electronic configuration, can be switched from a diamagnetic low-spin state (LS, $S = 0$, $t_{2g}^6 e_g^0$) to a paramagnetic high-spin state (HS, $S = 2$, $t_{2g}^4 e_g^2$). Weak continuous wave (cw) laser irradiation at low temperature is known as an efficient way for controlling SCO materials by light. By choosing the appropriate excitation wavelength, it is possible to selectively populate the HS state light-induced excited spin-state trapping (LIESST) or LS state (reverse-LIESST) (Hauser, 1986) which are long-lived in solids below a characteristic T_{LIESST} temperature (Létard *et al.*, 1999) and transient above (Lorenc *et al.*, 2009 and Lorenc *et al.*, 2012). In solution, the photoinduced HS state is transient at ambient temperature, and pump-probe studies were used to unveil the ultrafast molecular switching and explore the intersystem crossing (ISC) dynamics. The use of complementary probes, sensitive to different degrees of freedom, strongly help investigating both ultrafast electronic and structural dynamics (Gawelda *et al.*, 2007; Consani *et al.*, 2009; Bressler *et al.*, 2009; Cannizzo *et al.*, 2010; Zhang *et al.*, 2014; Marino *et al.*, 2014; and Auböck and Chergui, 2015). LIESST in molecular solids shows very similar features, and it is well established that the strong electron-structural coupling plays a central role in the photo-induced trapping of the HS state (van Veenendaal *et al.*, 2010; Cammarata *et al.*, 2014; Bertoni *et al.*, 2015a; and Bertoni *et al.*, 2015b). However, the strong interest of performing ultrafast LIESST in the solid state resides in the active nature of the crystalline solid: the constituting molecules can switch during the complex out-of-equilibrium pathway under the effect of lattice pressure or heating (Lorenc *et al.*, 2009; Lorenc *et al.*, 2012; Kaszub *et al.*, 2013; Marino *et al.*, 2015; and Bertoni *et al.*, 2015c). However, the associated energy transfer process from the absorber molecule to its crystalline environment was not investigated thus far. Here, we study the elementary electronic and structural processes involved during LIESST in the SCO material $[Fe(PM\text{-}AzA)_2(NCS)_2]$. For understanding the molecule-to-lattice energy transfer, we compare the photoresponse in $[Fe(PM\text{-}AzA)_2(NCS)_2]$ crystals with the dynamics of solid solution crystals where these SCO molecules are diluted in a passive $[Zn(PM\text{-}AzA)_2(NCS)_2]$ matrix.

II. EXPERIMENT

A. Sample description and steady state conversions

The molecular structure of the SCO compound $Fe(PM\text{-}AzA)_2(NCS)_2$ (cis-bis(thiocyanato) bis[(N-2′-pyridylmethylene)–4-(phenylazo)aniline]), as obtained by X-ray diffraction (Guionneau *et al.*, 1999), is represented in Fig. 1. This Fe^{II} system of d^6 electronic configuration undergoes a spin-crossover from a diamagnetic LS ($S = 0$) to a paramagnetic HS ($S = 2$) state (Létard *et al.*, 1999 and Guionneau *et al.*, 1999). It is monitored in Fig. 1(a) with magnetic susceptibility (χ_M) measurements. The $\chi_M T$ product gives direct information on the spin state and shows a smooth spin crossover centered at $T_{(1/2)} = 184$ K, typical of noncooperative systems (Ksenofontov *et al.*, 1998 and Guionneau *et al.*, 1999). Several techniques sensitive to different degrees of freedom can probe the spin state switching (Halcrow, 2013). It is well established with ligand field theory that the change of spin state is associated with an important reorganization of the ligand, bounded here by nitrogen atoms to the Fe.

In this family of SCO compounds, the main structural deformation of the FeN_6 octahedron is the change of the average $Fe-N$ distance, from $\langle Fe-N\rangle_{LS} \approx 1.97$ Å to $\langle Fe-N\rangle_{HS} \approx 2.16$ Å revealed by X-ray diffraction (Marchivie *et al.*, 2003 and Guionneau *et al.*, 2012). Therefore, X-ray absorption near edge spectroscopy (XANES) at the Fe^{II} K-edge can be used to monitor the structural reorganization accompanying the SCO (Briois *et al.*, 1995), and the maximum change is observed around 7125 eV (Bressler *et al.*, 2009 and Cammarata *et al.*, 2014). Fig. 1(b) shows that the thermal equilibrium spin-crossover can be monitored by the change of X-ray absorption spectroscopy (XAS) measured at 7215 eV. In addition, the change of electronic distribution is associated with a color change of the material and, consequently, the spin state conversion can also be monitored with optical measurements (Marino *et al.*, 2013 and Goujon *et al.*, 2008). Fig. 1(c) reports the overall reflectivity change with temperature, and it is clear that these three measurements, probing a similar thermal SCO, give complementary fingerprints of the SCO phenomenon. They also prove the occurrence of the photo-switching due to 830 nm light excitation (Figs. 1(a) and 1(c)) below $T_{LIESST} = 44$ K in this compound (Létard *et al.*, 1999). We note a smaller

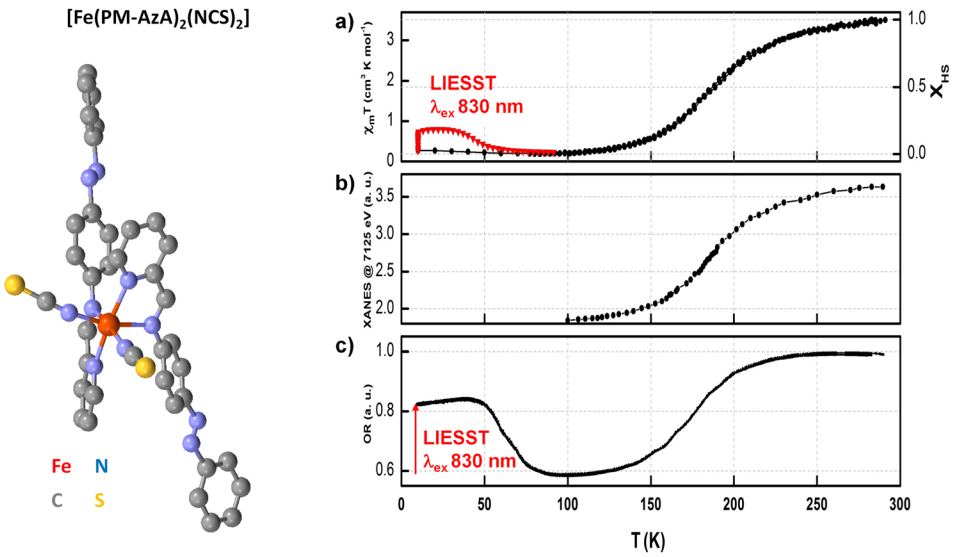

FIG. 1. Thermal spin crossover of the $[Fe(PM\text{-}AzA)_2(NCS)_2]$ compound (top) monitored with the evolution of (a) χ_M.T product, (b) X-ray absorption at 7125 eV, and (c) total optical reflectivity. The increase of χ_m. T and OR under cw light excitation at 830 nm in (a) and (c) is related to the long-lived LIESST phenomenon at low temperature.

change of magnetic susceptibility after photoexcitation at low temperature, compared to the thermal change (Fig. 1(a)), which is due to the rather thick powder sample used compared to the laser penetration depth, giving an overall limited fraction of photo-switched molecules (≈20%). Diffuse optical reflectivity (OR) data (Fig. 1(c)) probing mostly the surface show a greater fraction of molecules in the photoinduced HS state. These conventional techniques are too slow for investigating the photoswitching dynamics on the time scales of elementary processes, which typically fall in the sub-picosecond range. Here, we use two complementary femtosecond pump-probe techniques: optical spectroscopy and X-ray absorption. The $[Fe(PM\text{-}AzA)_2(NCS)_2]$ crystals appear fully dark, and optical transmission measurements cannot be performed in the visible range (VIS) (Marino *et al.*, 2013) but only in the near-infrared region (NIR) where 50 μm thick crystals become more transparent. Fig. 2(a) shows that because of this high absorption, the diffuse OR of the pure HS $[Fe(PM\text{-}AzA)_2(NCS)_2]$ is weak below 1200 nm. The changes in the VIS part of the OR spectrum measured on single crystals (Marino *et al.*, 2013) constitute a nice fingerprint of the SCO (Fig. 2(b)), as observed at thermal equilibrium in the spectral region of interest (630 nm–750 nm). An isosbestic point is evidenced around 690 nm. The OR increases during the

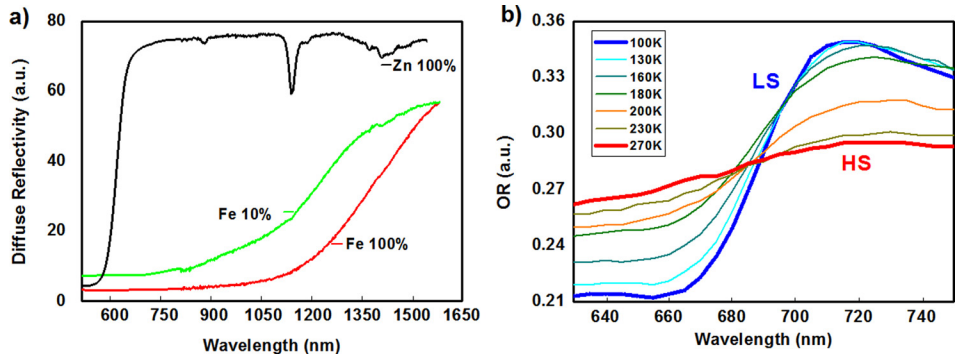

FIG. 2. (a) Diffuse reflectivity spectra collected on powders of $[Fe(PM\text{-}AzA)_2(NCS)_2]$ (red solid line), $[Zn_{0.9}Fe_{0.1}(PM\text{-}AzA)_2(NCS)_2]$ (green solid line) and $[Zn(PM\text{-}AzA)_2(NCS)_2]$ (black solid line) crystals. (b) Optical reflectivity spectra of a $[Fe(PM\text{-}AzA)_2(NCS)_2]$ single crystal acquired at different temperatures during the SCO from pure LS (100 K) and HS (270 K) states.

LS → HS switching below 690 nm, whereas it decreases above. The absorption decreases when the $[Fe(PM\text{-}AzA)_2(NCS)_2]$ molecules are diluted in a $[Zn(PM\text{-}AzA)_2(NCS)_2]$ crystalline matrix. Usually, such dilution of SCO molecules into isostructural lattice, which show no spin transitions, is used to modulate the coupling of the SCO molecule to the lattice and shifting phase transition to higher or lower temperature through the chemical pressure effect (Hauser, 2004). Here, we take advantage of the optical properties of the matrix to study LIESST, because the Zn-based molecules of $3d^{10}$ electronic configuration are optically silent in the 550–1050 nm, as confirmed by the OR diffuse spectra of the pure Zn compound. These Zn-based molecules adopt the same crystal structure as Fe-based ones, but do not present any spin crossover (Guionneau *et al.*, 2012). Consequently, the optical changes observed in the $[Zn_{0.9}Fe_{0.1}(PM\text{-}AzA)_2(NCS)_2]$ materials are only attributed to its constituting $[Fe(PM\text{-}AzA)_2(NCS)_2]$ SCO molecules.

All these specific optical properties can be explained by an accurate description of excited states, and the time dependent density functional theory (TD-DFT) approach is an excellent tool (Martin, 2003). The natural transition orbitals (NTOs) account for hole–particle pairs and can be used to interpret the excited states corresponding to the absorption of light. TD-DFT as implemented in the Gaussian 09 package (Gaussian 09, 2009) was applied for obtaining the NTO of the LS and HS $[Fe(PM\text{-}AzA)_2(NCS)_2]$ as well as $[Zn(PM\text{-}AzA)_2(NCS)_2]$ starting from geometry optimized molecule with b3lyp/lanl2dz hybrid functional–basis set. Fig. 3(a) shows the calculated oscillator strength change between LS and HS $[Fe(PM\text{-}AzA)_2(NCS)_2]$. The main features are the appearance of an absorption band above 1500 nm in the HS state, which is attributed to d-d transition from t_{2g}-like to e_g-like orbitals as shown by the NTO in Fig. 3(b). The LS d-d band is around 1200 nm in the LS state, where the ligand field is higher. The d-d transition in an $Fe\text{-}N_6$ Oh symmetry are strictly forbidden, but the $[Fe(PM\text{-}AzA)_2(NCS)_2]$ molecule in the crystal lies in general position (its point symmetry is C_1) and the FeN_6 core is not exactly octahedral, with 6 different Fe-N bonds (in the 1.94–1.98 Å range) and N-Fe-N angles different from 90° (in the 80°–93° range). In the LS state, the calculated oscillator strength of the d-d transitions is weak. In addition, because of the low symmetry, the t_{2g}-like orbitals are no more degenerate (this is also true for the 2 e_g-like orbitals) as schematically shown in the energy diagram (Fig. 3(b)). Consequently, different t_{2g}-like → 2 e_g-like transitions are calculated and the ones with strongest oscillator strength are shown at 1166 nm, 1236 nm, and 1250 nm (blue bars in Fig. 3(a) and blue arrows in Fig. 3(b)). In average, the d-d splitting is 10Dq ≈ 1.02 eV. We used such d-d transition in another SCO solid to induced the LS-to-HS photoswitching (Marino *et al.*, 2014). In the HS state, the deviation from Oh symmetry of the FeN_6 core is larger (Guionneau *et al.*, 1999 and Buron-Le Cointe *et al.*, 2012) for the Fe-N bonds (in the 2.06–2.27 A range) and the N-Fe-N angles from 90° (in the 74°–99° range). Consequently, the t_{2g}-like → 2 e_g-like transitions are stronger and shift to lower energy because of the 0.2 Å Fe-N elongation. The strongest t_{2g}-like → 2 e_g-like transitions are calculated at 1085 nm, 1450 nm, and 1650 nm (Figs. 3(a) and 3(b)), and

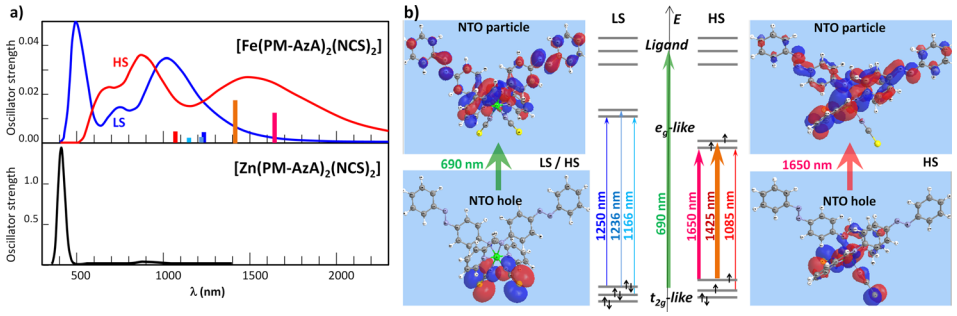

FIG. 3. (a) The TD-DFT calculated absorbance spectra for LS, HS, and Zn compounds. (b) At 690 nm NTO of hole and particle correspond to transitions from t_{2g}-like to L-like orbitals as shown here for the LS state (left) and at 1650 nm from t_{2g}-like to e_g-like orbitals for HS state only (right).

in average, the d-d splitting is around 0.92 eV. Therefore, the average decrease of the ligand field from the LS to the HS states is $D_{10Dq} = 0.1$ eV.

The calculated absorption change from LS to HS states (decreasing above 600 nm and increasing below) is also in agreement with the reflectivity change reported in Fig. 2(a), even though the isosbestic point is shifted by 90 nm with respect to our observations. The optical transitions around the isosbestic point (690 nm) correspond to metal to ligand charge-transfer (MLCT) transition, both for LS and HS states, as illustrated by the NTO shown in Fig. 3(b). The optical absorption of $[Zn(PM\text{-}AzA)_2(NCS)_2]$ is calculated to be very low in the 500–800 nm range, in agreement with the high reflectivity in Fig. 2(a), confirming that this compound is optically silent in this range. These optical results at thermal equilibrium are of importance for the time-resolved analysis performed hereafter.

B. Experimental conditions for femtosecond studies

The optical pump-probe experiments were configured in NIR-transmission and VIS-reflection geometry with a quasi-collinear configuration of pump and probe beams. The temporal evolution of Optical Density (OD) and OR were, respectively, obtained from the relative change of transmitted and reflected probe signals. The LS-to-HS photoswitching dynamics was first investigated on pure $[Fe(PM\text{-}AzA)_2(NCS)_2]$ single crystals (with typical dimensions of $(500 \pm 50) \times (70 \pm 5) \times (50 \pm 5)$ μm^3) and then on $[Zn_{0.9}Fe_{0.1}(PM\text{-}AzA)_2(NCS)_2]$ crystals with 10% of Fe molecules diluted in a passive zinc matrix. The sample temperature was controlled with a standard liquid nitrogen cryostream (Oxford Instruments Cryojet) and set for all experiments at 130 K to allow the HS-to-LS back relaxation within less than 1 ms (probe repetition rate of 1 kHz for the stroboscopic acquisition). For the optical experiments, two monochromatic ultrashort laser pulses of the duration of ∼40 fs generated with two optical parametric amplifiers (OPAs) were used as pump and probe leading to an overall instrumental response function (IRF) on the order of ∼80 fs. The pump wavelength was set to 800 nm on a MLCT band (where it efficiently induces LS-to-HS conversion as shown in Fig. 1) with an excitation density of 0.4 mJ/mm^2, typically switching 1%–2% of the molecules in the crystal (Lorenc *et al.*, 2012 and Collet *et al.*, 2012). The photo-response of such SCO materials is linear on the ps timescale with the excitation energy per pump pulse (Bertoni *et al.*, 2015a; 2015b; 2015c; and Marino *et al.*, 2015) and the data presented here were collected well below the sample damage (found around 1.0–1.5 mJ/mm^2). Data treatment involved iterative fitting of single/double exponential test functions convoluted with a Gaussian IRF of 80 fs. The residual oscillations observed in the OR curves were treated with a time dependent fast Fourier transform (FFT) analysis, in order to highlight the activation time of inter- and intra-molecular modes. For time scans up to 8 ps, we used a smoothing procedure above 1 ps, with a 200 fs time window (10 experimental time steps) for increasing the signal to noise ratio and showing better the 1.25 ps modes.

Time-resolved X-ray absorption measurements were performed at the XPP (X-ray pump-probe) end station of the LCLS X-FEL (X-ray Free Electron Laser) in Stanford, USA (Chollet *et al.*, 2015). For this experiment, ∼50 fs pump laser pulses, also centered at 800 nm, were used with an excitation density of 0.5 mJ/mm^2. The change in XAS was recorded with ∼30 fs X-ray probe pulses centered at 7125 eV. This energy is sensitive to the changes accompanying the SCO, as observed during the thermal crossover (Fig. 1(c)), or in ultrafast studies in other SCO compounds (Bressler *et al.*, 2009 and Cammarata, 2014). The IRF of 110 (10) fs at FWHM was obtained with a X-ray/optical cross correlator designed to correct for the jitter between the optical and the X-ray laser pulses (Harmand *et al.*, 2013).

III. RESULTS

A. Ultrafast structural trapping of the HS state

The OR dynamical time (dt) traces, recorded at selected probe wavelengths and reported in Fig. 4(a), enable to track in real time the ultrafast LIESST dynamics. The single color pump-probe measurements obtained with the probe set at 640 nm, 690 nm, and 720 nm clearly

reproduce the optical fingerprints characteristic of the LS → HS switching (Fig. 2(b)), with an ultrafast OR increase at 640 nm and decrease at 720 nm as the oscillator strength changes from LS to HS states in this spectral region. On the other hand, time-resolved analysis around the isosbestic point (690 nm), where LS and HS states contribute equally, allows an isolated observation of the dynamics of the intermediate (INT) state(s) involved during the spin-state photo-switching. Such INT states, as the initially photoexcited ^{1}MLCT state ($t_{2g}^5 e_g^0 L^1$), are responsible for the transient reflectivity peak around dt = 0. An exponential fit, taking into account our 80 fs IRF, indicates that the INT state(s) decays toward the HS state within less than 50 fs. This peak is found of Gaussian shape, and its width is limited by our experimental time resolution. This 50 fs decay from the ^{1}MLCT (possibly together through other possible INT states) was also reported in other SCO compounds (Marino *et al.*, 2013; Cammarata *et al.*, 2014; and Auböck, 2015).

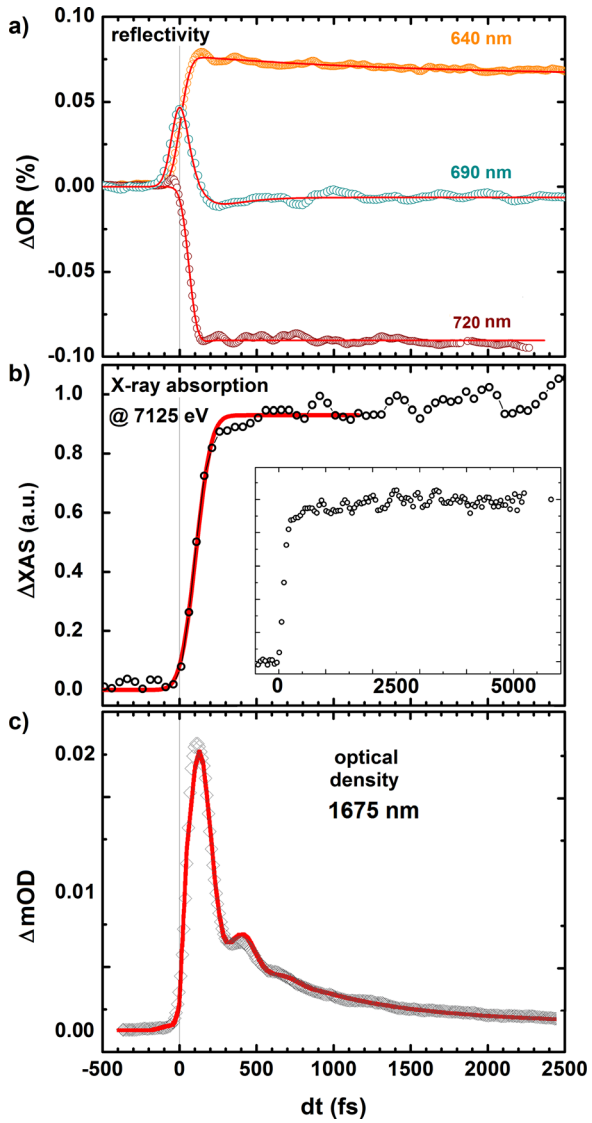

FIG. 4. Ultrafast dynamics in the 0–2500 fs range for the [Fe(PM-AzA) $_2$(NCS)$_2$] single crystal upon excitation in the MLCT bands at 800 nm (0.4–0.5 mJ/mm^2) observed by (a) two-color pump-probe reflectivity measurements with dynamical time traces for 640 nm, 690 nm, and 720 nm probe, (b) time-resolved change of XAS at 7125 eV after laser irradiation at 800 nm for the [Fe(PM-AzA)$_2$(NCS)$_2$], and (c) two-color pump-probe transmission measurements at 1675 nm. The fits (solid red lines) take into account the IRF of 80 fs for (a) and 110 fs for (b) and (c). The inset of (b) covers the 0–6 ps time window, whereas the inset of (c) covers the first ps.

Whereas optical measurements give mostly access to the change of electronic state, time-resolved X-ray absorption spectroscopy at the Fe^{II} K-edge enables to track in real time the structural reorganization around the FeN_6 core and especially to the change in $\langle$Fe-N$\rangle$ distance. Figure 4(b) reports the time course of the XAS measured at 7125 eV. The XAS increase at this energy is a clear characteristic fingerprint of the formation of the HS structure, as observed at thermal equilibrium (Fig. 1(c)) when $\langle$Fe-N$\rangle$ elongates from the equilibrium value of the LS state ($\langle Fe-N\rangle_{LS} \approx 1.97$ Å) to the one of the HS state ($\langle Fe-N\rangle_{HS} \approx 2.16$ Å) measured by X-ray diffraction (Guionneau *et al.*, 1999 and Marchivie *et al.*, 2003). An exponential fit convolved with our Gaussian IRF of 110 (10) fs allowed an accurate determination of the structural reorganization around Fe, with an elongation time constant $\tau_{\langle Fe\text{-}N\rangle} = 160$ (20) fs, similar to the one reported for other SCO molecules in crystal and solution (Bressler *et al.*, 2009; Lemke *et al.*, 2013; and Cammarata *et al.*, 2014). The signal remains constant for longer delays measured up to 6 ps (inset of Fig. 4(b)).

The optical transmission measurements in the spectral region probing the d-d transition of the HS state around 1200–1600 nm (Fig. 3) are also sensitive to the amplitude of the ligand field, which is modulated by the Fe-N distance (Bertoni *et al.*, 2015a). Figs. 4(c) and 5 report the time evolution of the OD, recorded in transmission geometry for different probe wavelengths in the 1200–1675 nm spectral range. The increase of absorption after photo-excitation of the LS state corresponds to the appearance of the HS d-d transitions. The OD increase of the HS state in these low energy bands results therefore from the d-d gap narrowing. Here, again an intermediate OD peak is observed around dt = 0 as the MLCT state also absorbs. The exponential fit of the time trace indicates that the decay towards the HS state occurs within 150 (20) fs. This timescale differs from the 50 fs decay of the MLCT state and may be associated with a contribution of an intermediate triplet state to this transient absorption. It is difficult to identify here because of its weak optical fingerprint, but it was directly observed on the pathway from MCLT to HS by X-ray emission techniques (Zhang *et al.*, 2014). This absorption change is governed by the t_{2g}-e_g gap narrowing as $\langle Fe-N\rangle$ elongates, with a time constant $\tau_{gap} = 150$ (20) fs, in good agreement with $\tau_{\langle Fe\text{-}N\rangle} = 160$ (20) fs measured by XAS. A slower 750 fs decay is also observed and associated with vibrational cooling already observed in preliminary measurements (Marino *et al.*, 2013). The apparent decay in Figs. 4(c) and 5 is therefore not associated with a decay of the HS state, as confirmed by constant XAS after 200 fs.

On top of this OD exponential decay, an oscillation also shows up at this probe wavelength. The insets of Fig. 5 show the oscillating component obtained by subtracting the exponential decay to the data. Since the MLCT peak decays within 150 fs, this 115 cm^{-1} oscillation (290 fs period), observed up to 1 ps, is therefore attributed to the HS state. It falls in the frequency range of the $\langle$Fe-N$\rangle$ breathing molecular mode reported in a similar SCO compounds

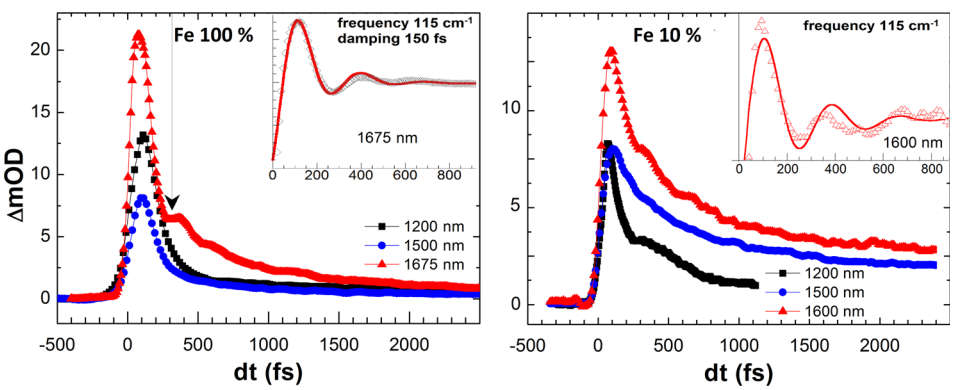

FIG. 5. Ultrafast dynamics in the 0–2500 fs range probed in the infra-red part on the HS d-d bands for the pure (100% Fe) $[Fe(PM-AzA)_2(NCS)_2]$ crystal (left) and for the 10% diluted $[Zn_{0.9}Fe_{0.1}(PM-AzA)_2(NCS)_2]$ crystal (right) after photo-excitation at 800 nm (0.4 mJ/mm^2); the insets show the oscillating part of the signal. For the Fe 100% compound, the fit at 1675 nm (red curve) gives a 115 cm^{-1} frequency and a 150 fs damping. For the fit at 1600 nm in the Fe 10% compound, the frequency was fixed to 115 cm^{-1} because of the noise limit and a 150 (50) fs damping was found.

(Baranovic and Babic, 2004; Ronayne *et al.*, 2006; Sousa *et al.*, 2013; Cammarata *et al.*, 2014; and Bertoni *et al.*, 2015a). As the ligand field (Fe-N distance) modifies the amplitude of the d-d absorption at 1675 nm, this mode is therefore very likely associated with the breathing of the Fe-N_6 core shell. Since the symmetry of this molecule is very low (the 6 Fe-N bonds are not symmetry equivalent), there is no proper breathing mode with the totally symmetric Fe-N stretching. However, the observed mode, probed around d-d transition, has Fe−ligand breathing character. The oscillation of the signal is rapidly damped, within 150 (30) fs. This effect may come from a damping of the amplitude of the molecular oscillations, but a dephasing of the response of the photo-switched molecules, resulting from energy transfer to other modes or to collision, is also very likely. It is interesting to underline that such a breathing mode cannot be attributed to impulsive Raman process in the ground LS state because on the one hand the LS breathing frequency is significantly higher (150 cm^{-1}) and on the other hand the LS state is silent at 1675 nm. This mode is also observed in our IR data in the diluted compound (Fig. 5), but the signal is more noisy due to the weak concentration of SCO molecules.

In addition to this mode, another vibration (67 cm^{-1}, 500 fs period) is observed for probing wavelengths around the isosbestic point (Fig. 6). Contrary to the 115 cm^{-1} mode, the 67 cm^{-1} mode it is not rapidly damped as few oscillations are observed during the first 2 ps. Since the absorption at this wavelength involves MLCT states (Fig. 3), this low frequency mode is very likely a molecular ligand torsion. This is also in agreement with calculations founding many ligand torsion modes in this frequency range (Baranovic and Babic, 2004; Ronayne *et al.*, 2006; Sousa *et al.*, 2013; Cammarata *et al.*, 2014; Bertoni *et al.*, 2015a; and Bertoni *et al.*, 2015b).

All these results are in good agreement with the recent literature reporting on the ultrafast LIESST for several Fe^{II} compounds, both in solution and solids (Cammarata *et al.*, 2014; Bertoni *et al.*, 2015a; and Auböck and Chergui, 2015). Since this LIESST dynamics is mostly the same for an isolated molecule in solution and for a molecule embedded in a single crystal, our results underline also that the ultrafast LIESST in SCO solids is strictly confined to a molecular response on the sub-ps timescale. Its MLCT state is short-lived (<50 fs), and the HS state is rapidly reached. Once in the HS potential, the molecular structure changes and the Fe-N bonds expand towards the equilibrium value. The breathing mode is then activated, and, because of the excess energy, the system oscillates in the HS potential where other modes, like ligand torsion, are activated. Our results are also consistent with the theoretical description of the LS → HS photo-switching process as resulting from the coherent activation and fast

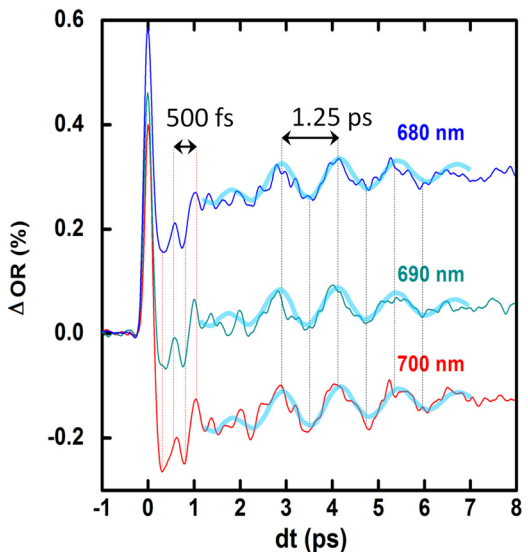

FIG. 6. Dynamical OR time traces recorded at 680 nm, 690 nm, and 700 nm after photoexcitation at 800 nm (0.4 mJ/mm^2) and showing in phase oscillations of the reflectivity signal. Thick cyan curves represent the fit to the data with a sine function multiplied with an increasing and decreasing exponential terms.

damping of the breathing mode, bringing and keeping the system in the HS potential (van Veenendaal *et al.*, 2010 and Cammarata *et al.*, 2014). We observe indeed that the 290 fs period breathing mode is highly damped within 150 fs. However, in Fig. 6, we can observe another oscillation with 1.25 ps period, activated later and persisting up to 8 ps. Such features were not observed in solution, and their nature is investigated in detail in Sec. III B.

B. Activation of coherent optical lattice phonon

From a first look at Fig. 6, it is possible to identify in the OR time traces the short MLCT peak, followed by two main oscillating components. During the first 2 ps, the weak 67 cm^{-1} oscillation (500 fs period) discussed above appears. Then the OR starts to oscillate with much higher amplitude, and these slower oscillations vanish around 8 ps. The fit of this mode, taking into account an exponential increase and decay of its spectral weight, is shown by the cyan thick lines (using the same parameters for the different time traces) and gives a ∼1.25 ps period (28 cm^{-1}). The oscillating component of Fig. 7 was extracted from the average bi-exponential fit describing decays of MLCT to HS state and the vibrational cooling (Marino *et al.*, 2013), and we plot in Fig. 7 its time dependent FFT (t-FFT) analysis. This analysis confirms the presence of the two different modes at around 67 cm^{-1} and 28 cm^{-1}. The 67 cm^{-1} mode is activated as the HS potential is reached and is observed in the 0–2 ps range and corresponds to molecular coherent oscillations in the photoinduced HS state. It is important to notice how the amplitude of the 28 cm^{-1} mode is maximum at 4 ps: it gradually increases around 2 ps and decreases until vanishing around 8 ps. We observe in Fig. 7 a spectral weight transfer from the 67 cm^{-1} to the 28 cm^{-1} modes. Such low frequency modes in the 30 cm^{-1} range are usually associated to large amplitude ligand torsion (Ronayne *et al.*, 2006). In molecular solids, this

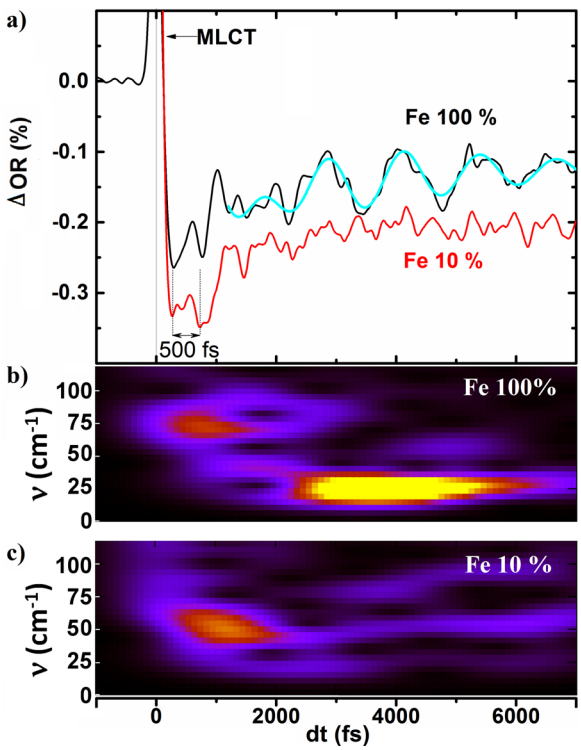

FIG. 7. (a) Comparison of the oscillating dynamics accompanying the ultrafast LIESST ($\lambda_{pump} = 800$ nm and $\lambda_{probe} = 700$ nm) for the the pure $Fe(PM-AzA)_2(NCS)_2$ crystal (black) and for the 10% diluted $[Zn_{0.9}Fe_{0.1}(PM-AzA)_2(NCS)_2]$ crystal (red). (b) Time dependent FFT analysis of the oscillating component of the OR at 700 nm showing the sequential activation of two different vibrations at 67 cm^{-1} and 28 cm^{-1} for the pure crystal (b) and the diluted compound (c). Thick cyan curves represent the fit to the data with a sine function multiplied with an increasing and decreasing exponential terms.

frequency range also corresponds to inter-molecular optical phonons, mixing molecular displacement and torsion (Uemura and Okamoto, 2010 and Servol *et al.*, 2015). It seems therefore difficult to discriminate from these results the nature of such a mode. Is it associated with the local oscillation of the photo-excited molecules or is it associated with an optical phonon?

For answering to this question, the same experiments were performed on solid solution crystals, where photoactive $[Fe(PM\text{-}AzA)_2(NCS)_2]$ molecules are diluted in a passive and optically silent crystalline matrix of $[Zn(PM\text{-}AzA)_2(NCS)_2]$ molecules. We used the solid solution $[Zn_{(1-x)}Fe_x(PM\text{-}AzA)_2(NCS)_2]$ with $x = 0.1$. By performing such time resolved analysis on diluted crystals, we hope to access only to the photo-response of the isolated photo-active Fe-based molecules and to learn more about its interaction with the crystalline environment. We should underline that a dilution of 10% means that one Fe-based molecule is in average isolated in a box surrounded by $2 \times 2 \times 2$ Zn-based molecules.

Figure 7 compares the dynamical time traces of optical reflectivity recorded for $\lambda_{probe} = 700$ nm and optical density in the IR for the pure and diluted crystal. The same experimental conditions were used with $\lambda_{pump} = 800$ nm, with a pump fluence of 0.4 mJ/mm^2. The photo-response of the diluted sample is similar to the one of the pure Fe compound. It starts with an ultrashort (<50 fs) MLCT peak partially shown in Fig. 6, zooming on the zone of interest, followed by the 500 fs (67 cm^{-1}) oscillations evident in the pure compound, and less pronounced in the diluted one. The lower oscillation amplitude in the diluted crystal is due to a smaller density of Fe-based molecules, and the higher noise for this record forbids an accurate extrapolation of the high frequency modes. The amplitude of the 28 cm^{-1} mode in the pure crystal is of the same order as the optical change between the first 500 fs and the signal around 2 ps. In the diluted crystal, we observe a similar optical change between 500 fs and 2 ps and consequently the signal/noise ratio looks good enough to observe the lattice phonon mode. Since it is not the case, we conclude that the 28 cm^{-1} oscillations are absent in the optical data, as confirmed by the time-dependent FFT (Figure 7). At that stage, we should keep in mind that such low frequency modes usually have lattice optical phonon character involving molecular bending, translation, and/or orientation (Ronayne *et al.*, 2006). In addition, the pure LS compound made of $[Fe(PM\text{-}AzA)_2(NCS)_2]$ molecules is absorbing at the 700 nm probe wavelength, and this absorption creating MLCT state can be modulated by molecular vibration. This is not the case for the $[Zn(PM\text{-}AzA)_2(NCS)_2]$ lattice matrix of the diluted compound, which is optically silent at 700 nm (Fig. 2). We therefore come to the conclusion that the 28 cm^{-1} vibration observed only in the pure compound is a lattice optical phonon mode.

IV. DISCUSSION

The results reported here give essential insight on the LIESST process in crystals and are complementary to ultrafast studies of LIESST at the molecular level performed for molecules in solution. Regarding the LIESST phenomenon itself, the use of complementary probes (optics and X-ray) allowed to determine the temporal evolution of the electronic and structural degrees of freedom at the molecular scale. The results underline that during LIESST the electronic and structural degrees of freedom are strongly coupled and evolve in sequential steps. A global picture schematically describing the photophysics mechanism of LIESST is represented in Fig. 8(a), with different potential energy curves representing the main electronic states of the system. After photoexcitation of the LS molecular state, the system reaches the ^{1}MLCT state, which decays within less than 50 fs, as observed with optical reflectivity around the HS/LS isosbestic point sensitive to this intermediate state. As the less bonding HS potential is rapidly reached, a new equilibrium $\langle$Fe-N$\rangle$ bond length is defined and its elongation occurs, as observed with time resolved XAS (Fig. 3(b)) and IR optical spectroscopy (sensitive to the average HS t_{2g}–e_g gap). This average bond elongation occurs within $\tau_{\langle Fe\text{-}N\rangle} \sim 160$ fs, and activates the intramolecular Fe-ligand stretching mode as the molecule oscillates in its new HS potential. Since this HS state is reached on a timescale corresponding typically to a half vibrational period of the Fe-N breathing mode, any intermediate state cannot be structurally relaxed and therefore can only serve as dynamically mixed mediators. These results reported here in the $[Fe(PM\text{-}AzA)_2(NCS)_2]$ SCO

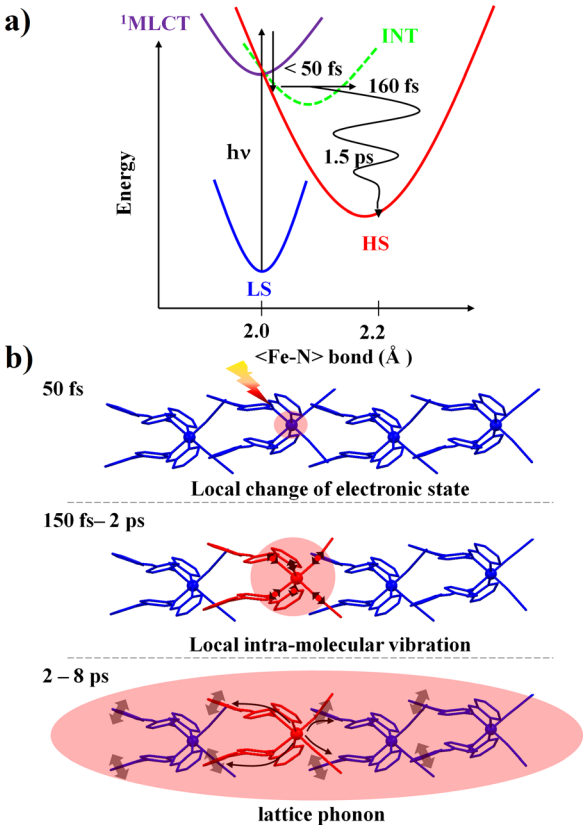

FIG. 8. (a) Schematic representation of the energy transfer from the absorber Fe-ion to the crystal lattice. A first laser excitation releases an excess of energy of ∼1.5 eV on the Fe-ion. Due to the electron-phonon coupling, the ultrafast $Fe-N$ bond elongation triggers coherent structural intra-molecular vibrations. A strong phonon-phonon coupling transfers the excess of energy from the molecule to the crystal lattice via phonon-phonon coupling. (b) Schematic summary of the ultrafast LIESST mechanism activated via LS → ^{1}MLCT laser excitation. Decay of the excited ^{1}MLCT state in less than 50 fs where possible intermediate (INT) states are involved in the intersystem crossing to the HS state. The HS electronic configuration implies a shift of the reaction coordinates to higher ⟨Fe-N⟩ bond lengths. This elongation is measured to occur in ∼160 fs. The HS potential is reached in a vibrational excited state where the nonradiative vibrational cooling inside the HS potential to its bottom occurs in ∼1.5–2 ps. The pink ellipsoids schematically represent the redistribution of the energy initially deposited on the molecule.

solid find a common agreement with recent works reporting the fast population of the HS state (Gawelda *et al.*, 2007; Consani *et al.*, 2009; Bressler *et al.*, 2009; Marino *et al.*, 2013; Zhang *et al.*, 2014; and Marino *et al.*, 2014) and the consecutive coherent activation of different intramolecular molecular modes in the HS potential in solution (Consani *et al.*, 2009 and Auböck and Chergui, 2015) and in the solid state (Cammarata *et al.*, 2014; Bertoni *et al.*, 2015a; and Bertoni *et al.*, 2015b). Once in the HS potential, a nonradiative vibrational cooling occurs (Cannizzo *et al.*, 2010 and Bertoni *et al.*, 2012) and the energy is transferred to the surrounding medium. In their high time resolution measurements, Auböck and Chergui observed a 30–50 fs phase shift of the Fe-N stretching mode and interpreted this as the characteristic the arrival time in the HS potential. Our time resolution (80 fs) is not good enough to give such accurate numbers, but our results agree with such observation. What is new here with respect to previous ultrafast studies of LIESST is the evidence of the energy transfer from the absorber SCO molecule to its surrounding lattice, activating so an optical lattice phonon. It is this energy transfer which is responsible for lattice heating and drives the consecutive lattice expansion observed on ns timescale and the thermal population of the HS state observed on μs timescale (Lorenc *et al.*, 2012; Collet *et al.*, 2012; Bertoni *et al.*, 2015a; 2015b; 2015c; and Marino *et al.*, 2015). Such lattice modes are not activated immediately after photo-excitation: the phase shift of this mode optical lattice phonon mode (250 (40) fs) may be interpreted as an activation of the mode due to

molecular swelling, which occurs on similar timescale. However, since the intensity of this mode increases during the 4 first ps, the process responsible for its activation is probably a coupling of the molecular modes with the lattice modes. Indeed, the intra-molecular vibration and the optical lattice phonon look sequentially activated, with a spectral weight transfer from the $67\,cm^{-1}$ to the $28\,cm^{-1}$ modes. In the Zn matrix, the $28\,cm^{-1}$ lattice vibration is not observed when energy is transferred from the Fe SCO molecule to the passive Zn-based lattice. This is due to the fact that the Zn-based lattice is optically silent, prohibiting so the observation of this mode. This result confirms that such vibrations are located on the lattice surrounding the absorber molecule and corresponds to optical lattice phonons. Considering the great deal of modes in the few tens of cm^{-1} in molecular crystals, it might seem surprising that only a particular one is present. We attribute this observation to the selectivity of the probe rather than a selective excitation process. Indeed, as discussed above, light at 690 nm should involve a transition to the ligand orbitals, thus being sensitive to the lattice vibrations coupled to the ligand torsion. Supporting this idea is the observation (in similar Fe^{III} compounds) of different lattice modes at different probe wavelengths (Bertoni *et al.*, 2015a; 2015b; and 2015c). One should also note that lattice modes at higher frequencies are probably excited as well. However, the energy transfer from the molecule to the lattice is longer than the oscillation periods of these modes, which are not activated coherently and consequently do not modulate the time-resolved signal.

Figure 8(b) is a schematic representation of this process following the molecular LIESST described above. One more time, we underline that the pump pulse locally photoswitches within a fragment of time the absorbing Fe-based molecules in the crystal. As these undergo LIESST, the HS potential is reached with an excess of energy in the order of 1–2 eV. The population of the antibonding e_g orbitals leads to a reorganization of the FeN_6 octahedron, occurring beyond a doubt within 160 fs, which in turn triggers the coherent activation of intra-molecular vibrations during the first 2 ps, also observed in the IR for the diluted compound (Fig. 5). As the molecule couples to its environment via intermolecular contacts, the vibrational relaxation of the HS state occurs and a coherent optical phonon of the lattice surrounding the photoexcited molecules is activated.

These findings evidence that the photo-switched SCO molecule in the crystal rapidly equilibrates with the environment, transferring within ~2 ps the energy (released on the molecule by the laser pulse) to the lattice. Since the lattice modes are coherently activated, the mechanism involved in the process is very likely a coupling between the intra-molecular modes and the lattice modes. Indeed, phonon−phonon coupling is known as an efficient way to transfer energy between different vibration modes (Uemura and Okamoto, 2010 and Fröst *et al.*, 2011). This process is of high importance for SCO solids as it is established that lattice expansion, induced here by its resulting heating (Collet *et al.*, 2012), can drive low spin to high spin transformation through the elastic coupling of the SCO molecules mediated by the lattice (Spiering *et al.*, 1982; Lorenc *et al.*, 2009; and Enachescu *et al.*, 2009).

ACKNOWLEDGMENTS

This work was supported by Institut Universitaire de France, Rennes Métropole, ANR (ANR-13-BS04-0002), Centre National de la Recherche Scientifique (CNRS) (PEPS SASLELX), and Fonds Européen de Développement Régional (FEDER). A.M. thanks CNRS and Région Bretagne for Ph.D. funding (COMMAND). Portions of this research were carried out at the Linac Coherent Light Source (LCLS) at SLAC National Accelerator Laboratory. LCLS is an Office of Science User Facility operated for the U.S. Department of Energy Office of Science by Stanford University.

Auböck, G. and Chergui, M., "Sub-50-fs photoinduced spin crossover in $[Fe(bpy)3]^{2+}$," Nat. Chem. **7**, 629–633 (2015).
Baranovic, G. and Babic, D., "Vibrational study of the Fe(phen)2(NCS)2 spin-crossover complex by density-functional calculations," Spectrochem. Acta, Part A **60**, 1013 (2004).
Barbara, P. F., Walker, G. C., and Smith, T. P., "Vibrational modes and the dynamic solvent effect in electron and proton transfer," Science **256**, 975 (1992).

Bertoni, R., Cammarata, M., Lorenc, M., Matar, S. F., Leťard, J.-F., Lemke, H. T., and Collet, E., "Ultrafast light-induced spin-state trapping photophysics investigated in Fe(phen)2(NCS)2 spin-crossover crystal," Acc. Chem. Res. **48**, 774–781 (2015a).
Bertoni, R., Lorenc, M., Laisney, J., Tissot, A., Moreac, A., Matar, S. F., Boillot, M.-L., and Collet, E., "Femtosecond spin-state photo-switching dynamics in an FeIII spin crossover solid accompanied by coherent structural vibrations," J. Mater. Chem. C **3**, 7792–7801 (2015).
Bertoni, R., Lorenc, M., Tissot, A., Boillot, M.-L., and Collet, E., "Femtosecond photoswitching dynamics and microsecond thermal conversion driven by laser heating in FeIII spin-crossover solids," Coord. Chem. Rev. **282–283**, 66–76 (2015c).
Bertoni, R., Lorenc, M., Tissot, A., Servol, M., Boillot, M.-L., and Collet, E., "Femtosecond spin-state photo-switching of molecular nanocrystals evidenced by optical spectroscopy," Angew. Chem., Int. Ed. **51**, 7485–7489 (2012).
Bressler, C., Milne, C., Pham, V.-T., El Nahhas, A., van der Veen, R. M., Gawelda, W., Johnson, S. L., Grolimund, D., Kaiser, D., Borca, C. N., Ingold, G., Abela, R., and Chergui, M., "Femtosecond XANES study of the light-induced spin crossover dynamics in an iron(II) complex," Science **323**(5913), 489–492 (2009).
Briois, V., Moulin, C., Sainctavit, P., Brouder, C., and Flank, A.-M., "Full multiple scattering and crystal field multiplet calculations performed on the spin transition FeII(phen)2(NCS)2 complex at the iron K and L2,3 X-ray absorption edges," J. Am. Chem. Soc. **117**, 1019–1026 (1995).
Buron-Le Cointe, M., Hébert, J., Baldé, C., Moisan, N., Toupet, L., Guionneau, P., Létard, J. F., Freysz, E., Cailleau, H., and Collet, E., "Intermolecular control of thermoswitching and photoswitching phenomena in two spin-crossover polymorphs," Phys. Rev. B **85**, 064114 (2012).
Cammarata, M., Bertoni, R., Lorenc, M., Cailleau, H., Di Matteo, S., Mauriac, C., Matar, S. F., Lemke, H., Chollet, M., Ravy, S., Laulhé, C., Létard, J.-F., and Collet, E., "Sequential activation of molecular breathing and bending during spin-crossover photoswitching revealed by femtosecond optical and X-ray absorption spectroscopy," Phys. Rev. Lett. **113**, 227402 (2014).
Cannizzo, A., Milne, C., Consani, C., Gawelda, W., Bressler, C., van Mourik, F., and Chergui, M., "Light-induced spin crossover in Fe(II)-based complexes: The full photocycle unraveled by ultrafast optical and X-ray spectroscopies," Coord. Chem. Rev. **254**(21–22), 2677–2686 (2010).
Chollet, M., Alonso-Mori, R., Cammarata, M., Damiani, D., Defever, J., Delor, J. T., Feng, Y., Glownia, J. M., Langton, J. B., Nelson, S., Ramsey, K., Robert, A., Sikorski, M., Song, S., Stefanescu, D., Srinivasan, V., Zhu, D., Lemke, H. T., and Fritz, D. M., J. Synchrotron Radiat. **22**, 503–507 (2015).
Chollet, M., Guerin, L., Unchida, N., Fukaya, S., Shimoda, H., Ishikawa, T., Matsuda, K., Hasegawa, T., Ota, A., Yamochi, H., Saito, G., Tazaki, R., Adachi, S.-I., and Koshihara, S., "Gigantic photoresponse in 1/4-filled-band organic salt (EDO-TTF)2PF6," Science **307**, 86–89 (2005).
Collet, E., Lemée-Cailleau, M. H., Buron-Le Cointe, M., Cailleau, H., Wulff, M., Luty, T., Koshihara, S., Meyer, M., Toupet, L., Rabiller, P., and Techerts, S., "Laser-induced ferroelectric structural order in an organic charge-transfer crystal," Science **300**, 612–615 (2003).
Collet, E., Lorenc, M., Cammarata, M., Guerin, L., Servol, M., Tissot, A., Boillot, M. L., Cailleau, H., and Buron-Le Cointe, M., "100 picosecond diffraction catches structural transients of laser-pulse triggered switching in a spin-crossover crystal," Chem.-Eur. J. **18**, 2051–2055 (2012).
Collet, E., Moisan, N., Baldé, C., Bertoni, R., Trzop, E., Laulhé, C., Lorenc, M., Servol, M., Cailleau, H., Tissot, A., Boillot, M. L., Graber, T., Henning, R., Coppens, P., and Buron-Le Cointe, M., "Ultrafast spin-state photoswitching in a crystal and slower consecutive processes investigated by femtosecond optical spectroscopy and picosecond X-ray diffraction," Phys. Chem. Chem. Phys. **14**, 6192 (2012).
Consani, C., Premont-Schwarz, M., Cannizzo, A., El Nahhas, A., van Mourik, F., Bressler, C., and Chergui, M., "Vibrational coherences and relaxation in the high-spin state of aqueous [Fell(bpy)3]2," Angew. Chem., Int. Ed. **48**, 39 (2009).
Elsaesser, T. and Kaiser, W., "Vibrational and vibronic relaxation of large polyatomic molecules in liquids," Annu. Rev. Phys. Chem. **42**, 83 (1991).
Enachescu, C., Stoleriu, L., Stancu, A., and Hauser, A., "Model for elastic relaxation phenomena in finite 2D hexagonal molecular lattices," Phys. Rev. Lett. **102**, 257204 (2009).
Fröst, M., Manzoni, C., Kaiser, S., Tomioka, Y., Tokura, Y., Merlin, R., and Cavalleri, A., "Nonlinear phononics as an ultrafast route to lattice control," Nat. Phys. **7**, 854 (2011).
Gao, M., Lu, C., Hubert, J.-R., Liul, C. L., Marx, A., Onda, K., Koshihara, S.-Y., Nakano, Y., Shao, X., Hiramatsu, T., Saito, G., Yamochi, H., Cooney, R. R., Moriena, G., Sciani, G., and Miller, D. R. J., "Mapping molecular motions leading to charge delocalization with ultrabright electrons," Nature **496**, 343–346 (2013).
Gaussian 09, Revision D.01, Frisch, M. J., Trucks, G. W., Schlegel, H. B., Scuseria, G. E., Robb, M. A., Cheeseman, J. R., Scalmani, G., Barone, V., Mennucci, B., Petersson, G. A., Nakatsuji, H., Caricato, M., Li, X., Hratchian, H. P., Izmaylov, A. F., Bloino, J., Zheng, G., Sonnenberg, J. L., Hada, M., Ehara, M., Toyota, K., Fukuda, R., Hasegawa, J., Ishida, M., Nakajima, T., Honda, Y., Kitao, O., Nakai, H., Vreven, T., Montgomery, J. A., Jr., Peralta, J. E., Ogliaro, F., Bearpark, M., Heyd, J. J., Brothers, E., Kudin, K. N., Staroverov, V. N., Kobayashi, R., Normand, J., Raghavachari, K., Rendell, A., Burant, J. C., Iyengar, S. S., Tomasi, J., Cossi, M., Rega, N., Millam, M. J., Klene, M., Knox, J. E., Cross, J. B., Bakken, V., Adamo, C., Jaramillo, J., Gomperts, R., Stratmann, R. E., Yazyev, O., Austin, A. J., Cammi, R., Pomelli, C., Ochterski, J. W., Martin, R. L., Morokuma, K., Zakrzewski, V. G., Voth, G. A., Salvador, P., Dannenberg, J. J., Dapprich, S., Daniels, A. D., Farkas, Ö., Foresman, J. B., Ortiz, J. V., Cioslowski, J., Fox, D. J., Gaussian, Inc., Wallingford, CT, 2009.
Gawelda, W., Cannizzo, A., Pham, V.-T., van Mourik, F., Bressler, C., and Chergui, M., "Ultrafast nonadiabatic dynamics of [FeII(bpy)3]2+ in solution," J. Am. Chem. Soc. **129**(26), 8199–8206 (2007).
Goujon, A., Varret, F., Boukheddaden, K., Chong, C., Jeftic, J., Garcia, Y., Naik, A. D., Ameline, J. C., and Collet, E., "An optical microscope study of photoswitching and relaxation in single crystals of the spin transition solid $[Fe(ptz)_6](BF_4)_2$, with image processing," Inorg. Chim. Acta **361**, 4055–4064 (2008).
Guionneau, P., Lakhloufi, S., Lemée-Cailleau, M.-H., Chastanet, G., Rosa, P., Mauriac, C., and Létard, J.-F., "Mosaicity and structural fatigability of a gradual spin-crossover single crystal," Chem. Phys. Lett. **542**, 52–55 (2012).

Guionneau, P., Létard, J.-F., Yufit, D. S., Chasseau, D., Bravic, G., Goeta, A. E., Howard, J. A. K., and Kahn, O., "Structural approach of the features of the spin crossover transition in iron(II) compounds," J. Mater. Chem. **9**, 985–994 (1999).
Gütlich, P. and Goodwin, H. A., *Spin Crossover in Transition Metal Compounds*, Topics in Current Chemistry Vol. 233, 234 and 235 (Springer, Berlin, 2004), p. 234. Available at http://www.springer.com/series/5103.
Halcrow, M. A., *Spin Crossover Materials: Properties and Applications* (Wiley, West Sussex, 2013), ISBN: 9781119998679.
Harmand, M., Coffee, R., Bionta, M. R., Chollet, M., Fritz, D. M., Lemke, H. M., Medved, N., Ziaja, B., Toleikis, S., and Cammarata, M., "Achieving few-femtosecond time-sorting at hard X-ray free electron lasers," Nat. Photonics **7**, 215–218 (2013).
Hauser, A., "Reversibility of light-induced excited spin state trapping in the Fe(ptz)6(BF4)2 and the Zn1-xFex(ptz)$_6$(BF$_4$)$_2$ spin-crossover systems," Chem. Phys. Lett. **124**, 6 (1986).
Hauser, A., "Light-induced spin-crossover and the high-spin → low-spin relaxation," Top. Curr Chem **234**, 155–198 (2004).
Jun, S., Yang, C., Kim, T. W., Isaji, M., Tamiaki, H., Ihee, H., and Kim, J., "Role of thermal excitation in ultrafast energy transfer in chlorosomes revealed by two-dimensional electronic spectroscopy," Phys. Chem. Chem. Phys. **17**, 17872–17879 (2015).
Kaszub, W., Buron-Le Cointe, M., Lorenc, M., Boillot, M. L., Servol, M., Tissot, A., Guerin, L., Cailleau, H., and Collet, E., "Spin-state photoswitching dynamics of the [(TPA)FeIII(TCC)]SbF6 complex," Eur. J. Inorg. Chem. **5–6**, 992–1000 (2013).
Kawakami, Y., Iwai, S., Fukatsu, T., Miura, M., Yoneyama, N., Sasaki, T., and Kobayashi, N., "Optical modulation of effective on-site Coulomb energy for the Mott transition in an organic dimer insulator," Phys. Rev. Lett. **103**, 066403 (2009).
Koshihara, S., "The LXIII Yamada conference on photo-induced phase transition and cooperative phenomena (PIPT3)," J. Phys.: Conf. Ser. **148**, 011001 (2009).
Ksenofontov, V., Levchenko, G., Spiering, H., Gütlich, P., Létard, J.-F., Bouhedja, Y., and Kahn, O., "Spin crossover behaviour under pressure of Fe(PM-L)$_2$(NCS)$_2$ compounds with substituted 2′-pyridylmethylene 4-anilino ligands," Chem. Phys. Lett. **294**, 545–553 (1998).
Lemke, H. T., Bressler, C., Chen, L. X., Fritz, D. M., Gaffney, K. J., Galler, A., Gawelda, W., Haldrup, K., Hartsock, R. W., Ihee, H., Kim, J., Kim, K. H., Lee, J. H., Nielsen, M. M., Stickrath, A. B., Zhang, W., Zhu, D., and Cammarata, M., "Femtosecond X-ray absorption spectroscopy at a hard X-ray free electron laser: Application to spin crossover dynamics," J. Phys. Chem. A **117**, 735 (2013).
Létard, J.-F., Capes, L., Chastanet, G., Moliner, N., Létard, S., Real, J. A., and Kahn, O., "Critical temperature of the LIESST effect in iron(II) spin crossover compounds," Chem. Phys. Lett. **313**, 115–120 (1999).
Levantino, M., Lemke, H. T., Schiró, G., Glownia, M., Cupane, A., and Cammarata, M., "Observing heme doming in myoglobin with femtosecond X-ray absorption spectroscopy," Struct. Dyn. **2**, 041713 (2015a).
Levantino, M., Schiró, G., Lemke, H. T., Cottone, G., Glownia, J. M., Zhu, D., Chollet, M., Ihee, H., Cupane, A., and Cammarata, M., "Ultrafast myoglobin structural dynamics observed with an X-ray free-electron laser," Nat. Commun. **6**, 6772 (2015b).
Lorenc, M., Balde, C. H., Kaszub, W., Tissot, A., Moisan, N., Servol, M., Buron-Le Cointe, M., Cailleau, H., Chasle, P., Czarnecki, P., Boillot, M., and Collet, E., "Cascading photoinduced, elastic, and thermal switching of spin states triggered by a femtosecond laser pulse in an Fe(III) molecular crystal," Phys. Rev. B **85**, 054302 (2012).
Lorenc, M., Hebert, J., Moisan, N., Trzop, E., Servol, M., Buron-Le Cointe, M., Cailleau, H., Boillot, M., Pontecorvo, E., Wulf, M., Koshihara, S., and Collet, E., "Successive dynamical steps of photoinduced switching of a molecular Fe(III) spin-crossover material by time-resolved X-ray diffraction," Phys. Rev. Lett. **103**, 028301 (2009).
Marchivie, M., Guionneau, P., Létard, J.-F., and Chasseau, D., "Towards direct correlations between spin-crossover and structural features in iron(II) complexes," Acta Crystallogr., Sect. B **59**, 479–486 (2003).
Marino, A., Buron-Le Cointe, M., Lorenc, M., Henning, R., DiChiara, A. D., Moffat, K., Bréfuel, N., and Collet, E., "Out-of-equilibrium dynamics of photoexcited spin-state concentration waves," Faraday Discuss. **177**, 363–379 (2015).
Marino, A., Chakraborty, P., Servol, M., Lorenc, M., Collet, E., and Hauser, A., "The role of ligand-field states in the ultrafast photophysical cycle of the prototypical iron(II) spin-crossover compound [Fe(ptz)6](BF4)2," Angew. Chem., Int. Ed. **53**, 3863–3867 (2014).
Marino, A., Servol, M., Bertoni, R., Lorenc, M., Mauriac, C., Létard, J. F., and Collet, E., "Femtosecond optical pump–probe reflectivity studies of spin-state photo-switching in the spin-crossover molecular crystals [Fe(PM-AzA)2](NCS)2," Polyhedron **66**, 123–128 (2013).
Martin, R., "Natural transition orbitals," J. Chem. Phys. **118**, 4775 (2003).
Okamoto, H., Ishige, Y., Tanaka, S., Kishida, H., Iwai, S., and Tokura, Y., "Photoinduced phase transition in tetrathiafulvalene-p-chloranil observed in femtosecond reflection spectroscopy," Phys. Rev. B **70**, 165202 (2004).
Ronayne, K. L., Paulsen, H., Höfer, A., Dennis, A. C., Wolny, J. A., Chumakov, A. I., Schünemann, V., Winkler, H., Spiering, H., Bousseksou, A., Gütlich, P., Trautwein, A. X., and McGarvey, J. J., "Vibrational spectrum of the spin crossover complex [Fe(phen)$_2$(NCS)$_2$] studied by IR and Raman spectroscopy, nuclear inelastic scattering and DFT calculations," Phys. Chem. Chem. Phys. **8**, 4685 (2006).
Rosspeintner, A., Lang, B., and Vauthey, E., "Ultrafast photochemistry in liquids," Annu. Rev. Phys. Chem. **64**, 247 (2013).
Schoenlein, R. W., Peteanu, L. A., Mathies, R. A., and Shank, C. V., "The first step in vision: Femtosecond isomerization of rhodopsin," Science **254**, 412–415 (1991).
Servol, M., Moisan, N., Collet, E., Cailleau, H., Kaszub, W., Toupet, L., Boschetto, D., Ishikawa, T., Moréac, A., Koshihara, S., Maesato, M., Uruichi, M., Shao, X., Nakano, Y., Yamochi, H., Saito, G., and Lorenc, M., "Local response to light excitation in the charge-ordered phase of (EDO−TTF)$_2$SbF$_6$," Phys. Rev. B **92**, 024304 (2015).
Sousa, C., de Graaf, C., Rudavskyi, A., Broer, R., Tatchen, J., Etinski, M., and Marian, C. M., "Ultrafast deactivation mechanism of the excited singlet in the light-induced spin crossover of [Fe(2,2'-bipyridine)$_3$]$^{2+}$," Chem. Eur. J. **19**, 17541–17551 (2013).

Spiering, H., Meissner, E., Koppen, H., Muller, E. W., and Gutlich, P., "The effect of the lattice expansion on high spin low spin transitions," Chem. Phys. **68**, 65–71 (1982).
Uemura, H. and Okamoto, H., "Direct detection of the ultrafast response of charges and molecules in the photoinduced neutral-to-ionic transition of the organic tetrathiafulvalene-p-chloranil solid," Phys. Rev. Lett. **105**, 258302 (2010).
van Veenendaal, M., Chang, J., and Fedro, A. J., "Model of ultrafast intersystem crossing in photoexcited transition-metal organic compounds," Phys. Rev. Lett. **104**(25), 067401 (2010).
Zhang, W., Alonso-Mori, R., Bergmann, U., Bressler, C., Chollet, M., Galler, A., Gawelda, W., Hadt, R. G., Hartsock, R. W., Kroll, T., Kjær, K. S., Kubiček, K., Lemke, H. T., Liang, H. W., Meyer, D. A., Nielsen, M. M., Purser, C., Robinson, J. S., Solomon, E. I., Sun, Z., Sokaras, D., van Driel, T. B., Vankó, G., Weng, T. C., Zhu, D., and Gaffney, K. J., "Tracking excited-state charge and spin dynamics in iron coordination complexes," Nature **509**(7500), 345–348 (2014).